

Copyright ©2010 by The American Physical Society

Reprinted from *PHYSICAL REVIEW B* **81**, 012304 (2010)

This material is posted here with permission of the APS Journal. Such permission of the APS Journal does not in any way imply APS Journal endorsement of any of the University of Verona (Italy)'s products or services. Internal or personal use of this material is permitted. However, permission to reprint/republish this material for advertising or promotional purposes or for creating new collective works for resale or redistribution must be obtained from the APS Journal by writing to [assocpub@aps.org](mailto:assocpub@aps.org)

## Local dynamical properties of crystalline germanium and their effects in extended x-ray absorption fine structure

Andrea Sanson\*

*Dipartimento di Informatica, Università degli Studi di Verona, Strada le Grazie 15, I-37134 Verona, Italy*  
(Received 23 October 2009; revised manuscript received 14 December 2009; published 22 January 2010)

The local dynamics of crystalline germanium has been investigated by molecular-dynamics simulations. The radial distribution functions of the first six coordination shells, as well as their parallel and perpendicular mean-square relative displacements, have been determined as a function of temperature. The agreement with the available extended x-ray absorption fine-structure data is very good. Original insights on the outer shells have been achieved. In particular, differently from the first shell, the bond thermal expansion of the outer shells is mainly due to the shift of the maximum of the distance distribution while the contribution of the distribution asymmetry is smaller than 15%.

DOI: [10.1103/PhysRevB.81.012304](https://doi.org/10.1103/PhysRevB.81.012304)

PACS number(s): 61.05.cj, 63.20.-e, 65.40.De

Extended x-ray absorption fine-structure (EXAFS) spectroscopy is one of the most powerful technique which gives the possibility of extracting original information on the local dynamical properties of crystals.<sup>1-4</sup> In particular, the nearest-neighbor EXAFS signal can be parameterized in terms of distribution of interatomic distances through the cumulant expansion method<sup>5,6</sup> in which the first four cumulants measure the average value ( $C_1^*$ ), the variance ( $C_2^*$ ), the asymmetry ( $C_3^*$ ), and the flatness ( $C_4^*$ ) of the distribution, respectively. EXAFS can also give information on the correlation of atomic thermal motion, measured by the mean-square relative displacement (MSRD), which is conveniently decomposed into its projections parallel and perpendicular to the average bond direction:<sup>7</sup>  $\langle \Delta u^2 \rangle = \langle \Delta u_{\parallel}^2 \rangle + \langle \Delta u_{\perp}^2 \rangle$ . The second cumulant of EXAFS corresponds to a good approximation to the *parallel* MSRD ( $C_2^* = \langle \Delta u_{\parallel}^2 \rangle$ ) (Ref. 6) while by comparing the thermal expansions measured by EXAFS and Bragg diffraction, one can obtain the *perpendicular* MSRD ( $\langle \Delta u_{\perp}^2 \rangle$ ), whose knowledge can give significant insights into the local vibrations responsible, for example, of negative thermal expansion.<sup>8</sup> In the case of germanium, the first shell perpendicular MSRD was determined by comparing the EXAFS and crystallographic thermal expansion.<sup>9</sup>

In spite of the recent advances in EXAFS interpretation, a deeper insight of the effects of atomic thermal motion on EXAFS still represents a basic problem not yet resolved. In this regard, a controversial issue concerns the relation between the thermal expansion of interatomic distances and the asymmetry of the corresponding distributions.<sup>10,11</sup> In the classical approximation, the distribution of distances can be expressed as a canonical average  $\rho(r) = e^{-V(r)/k_B T} / \int e^{-V(r)/k_B T} dr$ , where  $V(r)$  is a one-dimensional effective pair potential which depends on the statistically averaged behavior of all the atoms in the crystal and is, in principle, temperature dependent, both in position and shape. The EXAFS thermal expansion  $\Delta C_1^*$  thus depends not only on the asymmetry of the effective potential (i.e., on the asymmetry of the distance distribution) but also on its rigid shift, which originates from thermal vibrations perpendicular to the bond direction and possibly from other causes.<sup>6,12-14</sup>

A better understanding of this problem would enhance the potentialities of EXAFS, its accuracy, and avoid misinterpre-

tations. To this aim, theoretical calculations of the EXAFS thermal parameters, also independently from experimental data, are necessary. Important information could be obtained from the theoretical study of farther coordination shells, where an accurate analysis of experimental data has been up to now limited by multiple-scattering effects, which require an exceedingly large number of parameters to be fitted.

Some theoretical investigations were made on this matter. Classical Monte Carlo simulations of solid krypton suggest that the outer shells are much less asymmetric than the first one and the increase in the first cumulant nearly corresponds, for the outer shells, to the shift of the maximum position of the distribution.<sup>15,16</sup> The behavior of a van der Waals solid-like krypton can however hardly be generalized to other crystals. More recently, path-integral Monte Carlo calculations have shown that also in copper the asymmetry of the distance distribution is much larger for the first shell than for the outer shells while the temperature dependence of the minimum of the effective pair potential is not negligible and is different for different coordination shells.<sup>17</sup>

In this work, classical molecular-dynamics (MD) simulations have been performed in crystalline germanium from 100 to 700 K. The aims of the present study are (i) to reproduce the available experimental data measured by EXAFS and (ii) to gain original information on the local dynamics and radial distribution function of the outer coordination shells.

MD simulations have been performed by using the General Utility Lattice Program (GULP) code.<sup>18</sup> The radial distribution functions and the corresponding EXAFS cumulants have been calculated from MD trajectories by in-house developed software. A Stillinger-Weber-type interatomic potential<sup>19</sup> have been used. It is a combination of two-body and three-body potentials, previously employed for modeling the structure of solid phases of germanium and to calculate other crystal properties.<sup>20-22</sup> The potential parameters used in this work are the same of Ref. 20, except for parameter  $A$  set to 5.70 in order to obtain the third cumulant of the first shell more close to the experiment. The MD calculations have been done on a large simulation box, of  $6 \times 6 \times 6$  supercell dimension (432 atoms) with periodic boundary conditions. The cell parameter was adjusted at each temperature accord-

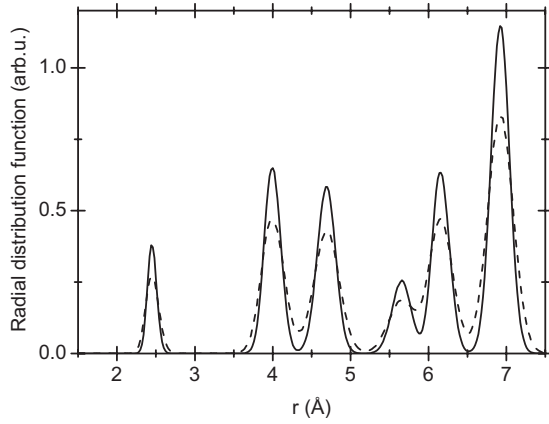


FIG. 1. Radial distribution function of the first six coordination shells at 300 K (solid line) and 600 K (dashed line).

ing to available crystallographic data<sup>23</sup> (an average linear coefficient of thermal expansion of  $5.9 \times 10^{-6} \text{ K}^{-1}$  was adopted). Integration of the Newton equations of motion was performed employing the Verlet Leapfrog algorithm<sup>24</sup> with a time step of 0.5 fs. At each temperature, the data for the calculation of the radial distribution functions have been collected for a total time of 5 ps after an initial equilibration time of 0.5 ps.

The total radial distribution function of the first six coord-

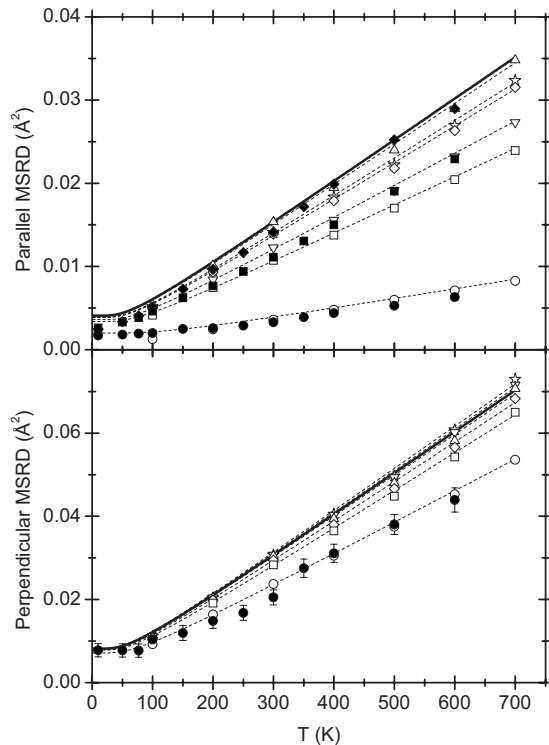


FIG. 2. Parallel MSRDS (top panel) and perpendicular MSRDS (bottom panel) for the first (circles), second (squares), third (diamonds), fourth (up triangles), fifth (down triangles), and sixth (stars) coordination shells. Dashed lines are the corresponding Einstein models. Closed symbols are the experimental MSRDS from EXAFS (Refs. 9 and 14). Black solid lines in the two panels are the uncorrelated parallel and perpendicular MSDs, respectively.

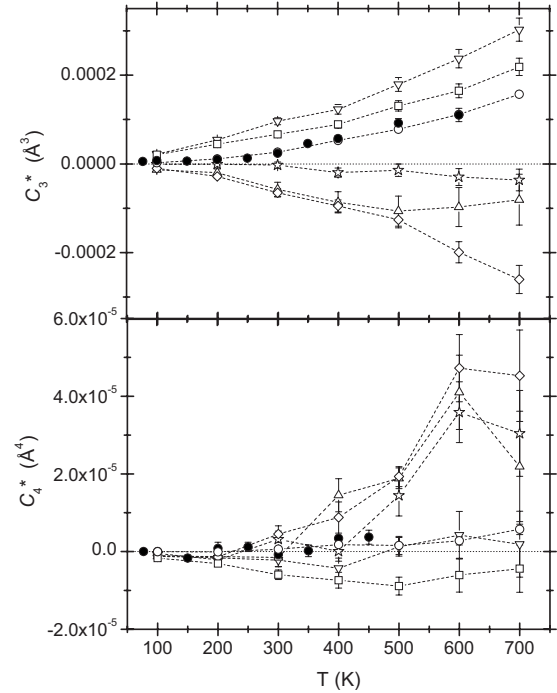


FIG. 3. Third cumulant (top panel) and fourth cumulant (bottom panel) for the first six coordination shells. Open symbols are the same of Fig. 2. Closed symbols are the experimental values for the first shell (Refs. 9 and 14). The dashed lines are guides to eye.

inations shells of germanium, calculated from the trajectories generated by MD, are shown in Fig. 1. For each shell, the first four cumulants have been calculated, as well as the maximum of the distribution, evaluated by a polynomial fit around the maximum position. Furthermore, the parallel and the perpendicular MSRDS [as well as the uncorrelated mean-square displacements (MSDs) of the atoms] have been calculated by the atomic displacements from the equilibrium positions, projected along the interatomic distance and on the perpendicular plane, respectively. For each shell, the difference between second cumulant and parallel MSRDS is negligible; the same is for the perpendicular MSRDS, obtained by comparing bond and crystallographic thermal expansion or evaluated from the projection of atomic displacements.

The parallel and perpendicular MSRDS obtained from the present study are shown in Fig. 2. The dashed lines are the corresponding Einstein models, whose frequencies were obtained by fitting MD data using the Einstein model in the classical limit.<sup>25–27</sup> In this way, the MSRDS can be estimated also at low temperatures, where classical MD simulations are known (in principle) to fail. The agreement between MD and EXAFS experiments<sup>9,14</sup> is very good, in particular, for the first shell. The small discrepancies in the second and third shells, no more than 10%, can be due to the presence of multiple-scattering effects in the EXAFS analysis. Also the uncorrelated mean-square displacement calculated by MD (black solid lines in Fig. 2) is in agreement with experimental data from x-ray diffraction,<sup>28</sup> where the parallel MSD (half of the perpendicular MSD) was measured about  $0.015 \text{ Å}^2$  at 300 K, and with recent *ab initio* calculations by Schowalter *et al.*<sup>29</sup>

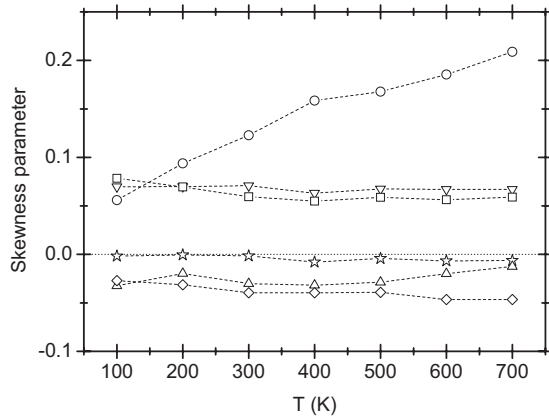


FIG. 4. Skewness parameter for the first six coordination shells. Symbols are the same of Fig. 2. The dashed lines are guides to eye.

The parallel MSRDR is smaller for the first shell than for the outer shells, indicating a stronger correlation. In the perpendicular directions, the correlation is less strong but again stronger for the first shell than for the outer shells, where the atomic motion is almost uncorrelated. At high temperatures, the anisotropy of relative vibrations, measured by the ratio  $\gamma = \langle \Delta u_{\perp}^2 \rangle / \langle \Delta u_{\parallel}^2 \rangle$ , is about 6.4 for the first shell, as a consequence of the considerable degree of correlation in the parallel direction. The agreement with the experiment is excellent.<sup>9</sup> For the outer shells,  $\gamma$  is within the range of about 2.0/2.7, therefore close to the case of parallel-perpendicular isotropy ( $\gamma=2$ ). The significant differences between first and

outer shells are entirely consistent with the behavior of III-V semiconductors, where nearest-neighbor bond bending is energetically favored over bond stretching and with the fact that there is no physical bond between atoms of the outer shells.<sup>30</sup>

The third and fourth cumulants for the first six coordination shells, calculated by MD, are shown in Fig. 3. The values for the first shell are in very good agreement with the experimental values measured by EXAFS.<sup>9,14</sup> The experimental values for the second and third shells are strongly affected by multiple scattering and so cannot be trusted. The third cumulant of the third, fourth, and sixth shells, calculated by MD, have negative values. A similar behavior was recently found for the second shell of copper by path-integral Monte Carlo calculations.<sup>17</sup> Although the origin of the negative third cumulant is not yet well understood, a correlation between third and fourth cumulants is observed in germanium: shells with a negative third cumulant display high values for the fourth cumulant; vice versa, shells with a positive third cumulant display a fourth cumulant close to zero.

The skewness parameter  $\beta = C_3^*/(C_2^*)^{3/2}$ , which measures the asymmetry of the distribution, is reported in Fig. 4 for the first six coordination shells. The asymmetry of first-shell distribution depends on temperature more strongly than outer shells. In addition, the outer-shell distributions are much less asymmetric than the distribution of the first shell, confirming previous findings for copper<sup>17</sup> and solid krypton,<sup>15,16</sup> where an “effective cancellation” of the asymmetric contribution was proposed for the outer shells. As a consequence, it can be concluded that the relevance of the third cumulant in EX-

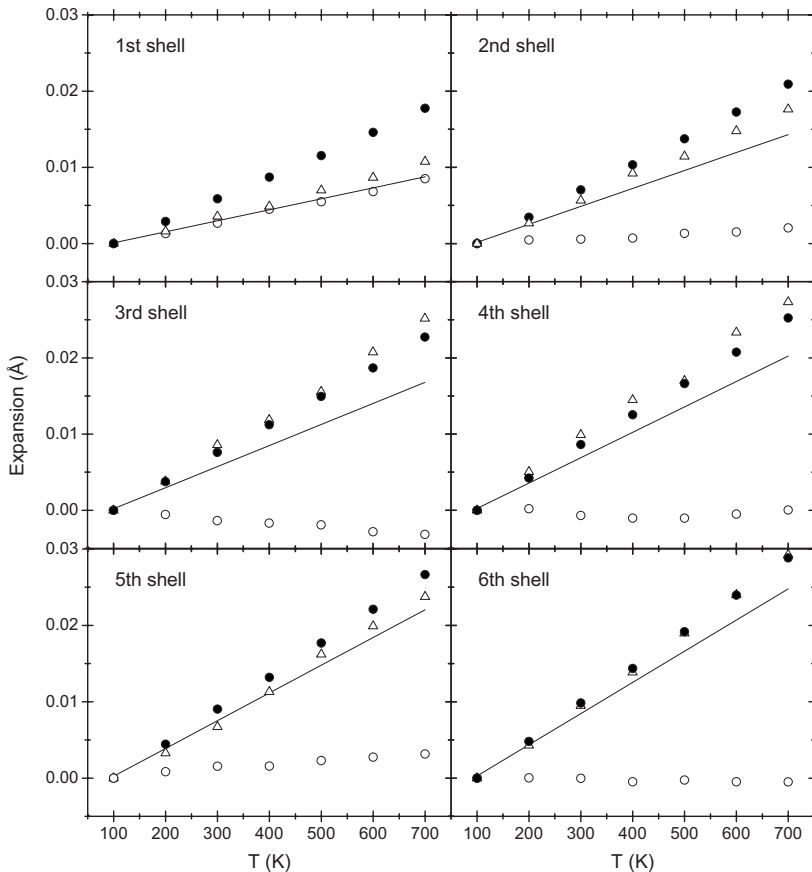


FIG. 5. Comparison between the bond thermal expansions measured by the first EXAFS cumulants (solid circles), the contribution due to the asymmetry of the distributions (open circles), and the shifts of the maximum of the distributions of distances of distributions (triangles). Solid lines are the crystallographic thermal expansions, here reported for comparison.

AFS analysis is smaller for the outer shells than for the first shell. On the contrary, for the first shell, the third cumulant cannot be neglected in the analysis, if accurate values of the first cumulant are sought.

For a diatomic system the bond thermal expansion, measured by the temperature variation  $\Delta C_1^*$  of the first EXAFS cumulant, is solely due to the asymmetry of the distance distribution, i.e., to the asymmetry of the interatomic pair potential. In this case,  $\Delta C_1^*$  can be evaluated from the second and third cumulants on the basis of a perturbative quantum approach that, in the classical limit, reduces to  $\Delta C_1^* = C_3^*/(2C_2^*)$ .<sup>31–33</sup> Differently, for a crystal, the bond thermal expansion  $\Delta C_1^*$  can also depend on a shift of the maximum of the distance distribution, which corresponds to a shift of the minimum of the effective pair potential.<sup>11,12</sup>

On this regards, the present MD study gives new information. For the first six shells of germanium, the bond thermal expansion has been calculated and compared to the shift of the maximum of the distribution, and with the contribution  $C_3^*/(2C_2^*)$  due to the distribution asymmetry (Fig. 5). For comparison, also the crystallographic thermal expansion is reported. For the first shell, the contribution due to the asymmetry is comparable to that from the rigid shift of the distribution and is connected to the high value of the skewness parameter or rather to the low value of the second cumulant (i.e., to the stronger correlation along the bond direction). On the contrary, for the outer shells, the bond thermal expansion

$\Delta C_1^*$  is almost entirely accounted for by the shift of the maximum of the distribution. The contribution due to the asymmetry is much weaker, about 10–15 % for the second, third, and fifth shells, no more than 2% for the fourth and sixth shells. As a result, a general relation between skewness parameter (i.e., third cumulant) and bond thermal expansion cannot be established nor with the crystallographic thermal expansion.

In conclusion, in this work, the local dynamics of the first six shells of crystalline germanium has been investigated by MD simulations. The agreement with the available experimental data, i.e., first four cumulants of the first shell and second cumulants of the second and third shells, is very good. In addition, significant information has been obtained on the outer shells. The distribution asymmetry for the outer shells is smaller than for the first shell; for the third, fourth, and sixth shells the asymmetry being even negative. The temperature dependence of the maximum of the distance distributions, i.e., of the minimum of the effective pair potential, is the main contribution to the bond thermal expansion, confirming previous investigations in face-centered-cubic crystals. Besides their interest from a basic research point of view, the present results should be considered to enhance the potentialities of EXAFS in the analysis of the outer shells.

The author is grateful to P. Fornasini for useful discussions, to J. D. Gale for supplying the GULP program package and advice, and to M. Giarola for CPU time.

\*andrea.sanson@univr.it

- <sup>1</sup>J. M. Tranquada and R. Ingalls, Phys. Rev. B **28**, 3520 (1983).
- <sup>2</sup>S. a Beccara *et al.*, Phys. Rev. Lett. **89**, 025503 (2002).
- <sup>3</sup>M. Vaccari *et al.*, Phys. Rev. B **75**, 184307 (2007).
- <sup>4</sup>S. I. Ahmed *et al.*, Phys. Rev. B **79**, 104302 (2009).
- <sup>5</sup>G. Bunker, Nucl. Instrum. Methods **207**, 437 (1983).
- <sup>6</sup>P. Fornasini *et al.*, J. Synchrotron Radiat. **8**, 1214 (2001).
- <sup>7</sup>P. Fornasini, J. Phys.: Condens. Matter **13**, 7859 (2001).
- <sup>8</sup>P. Fornasini *et al.*, Nucl. Instrum. Methods Phys. Res. B **246**, 180 (2006).
- <sup>9</sup>G. Dalba *et al.*, Phys. Rev. Lett. **82**, 4240 (1999).
- <sup>10</sup>F. D. Vila *et al.*, Phys. Rev. B **76**, 014301 (2007).
- <sup>11</sup>P. Fornasini *et al.*, Phys. Rev. B **70**, 174301 (2004).
- <sup>12</sup>O. Kamishima *et al.*, Solid State Commun. **103**, 141 (1997).
- <sup>13</sup>G. Dalba *et al.*, Phys. Rev. B **58**, 4793 (1998).
- <sup>14</sup>G. Dalba *et al.*, Phys. Rev. B **52**, 149 (1995).
- <sup>15</sup>A. Di Cicco, A. Filipponi, J. P. Itié, and A. Polian, Phys. Rev. B **54**, 9086 (1996).
- <sup>16</sup>T. Yokoyama *et al.*, Phys. Rev. B **55**, 11320 (1997).
- <sup>17</sup>S. a Beccara and P. Fornasini, Phys. Rev. B **77**, 172304 (2008).
- <sup>18</sup>J. D. Gale, J. Chem. Soc., Faraday Trans. **93**, 629 (1997).
- <sup>19</sup>F. H. Stillinger and T. A. Weber, Phys. Rev. B **31**, 5262 (1985).

- <sup>20</sup>K. Ding and H. C. Andersen, Phys. Rev. B **34**, 6987 (1986).
- <sup>21</sup>J. C. Noya *et al.*, Phys. Rev. B **56**, 237 (1997).
- <sup>22</sup>M. Posselt and A. Gabriel, Phys. Rev. B **80**, 045202 (2009).
- <sup>23</sup>Y. S. Touloukian *et al.*, *Thermophysical Properties of Matter* (Plenum, New York, 1977), Vol. 13.
- <sup>24</sup>M. Allen and D. Tildesley, *Computer Simulation of Liquids* (Clarendon, Oxford, 1991).
- <sup>25</sup>M. Vaccari and P. Fornasini, J. Synchrotron Radiat. **13**, 321 (2006).
- <sup>26</sup>A. Sanson, J. Synchrotron Radiat. **15**, 514 (2008).
- <sup>27</sup>In the classical limit, the Einstein model for the parallel and perpendicular MSRDS becomes  $k_B T / (4\pi^2 \mu \nu_{\parallel}^2)$  and  $k_B T / (2\pi^2 \mu \nu_{\perp}^2)$ , respectively. Because of the classical nature of MD data, the Einstein frequencies were obtained by these expressions.
- <sup>28</sup>N. M. Butt *et al.*, Acta Crystallogr. Sect. A **44**, 396 (1988).
- <sup>29</sup>M. Schowalter *et al.*, Acta Crystallogr. Sect. A **65**, 5 (2009).
- <sup>30</sup>C. S. Schnohr *et al.*, Phys. Rev. B **79**, 195203 (2009).
- <sup>31</sup>A. I. Frenkel and J. J. Rehr, Phys. Rev. B **48**, 585 (1993).
- <sup>32</sup>L. Wenzel *et al.*, Phys. Rev. Lett. **64**, 1765 (1990).
- <sup>33</sup>E. A. Stern *et al.*, Phys. Rev. B **43**, 8850 (1991).